Alcohol Exposure During the Brain Growth Spurt Alters Medial Prefrontal Cortex-Hippocampus Functional Connectivity During a Spatial Working Memory Task

by

Hailey Rosenblum

A thesis submitted to the Faculty of the University of Delaware in partial fulfillment of the requirements for the degree of Honors Degree in Neuroscience with Distinction

Spring 2023

Alcohol Exposure During the Brain Growth Spurt Alters Medial Prefrontal Cortex-Hippocampus Functional Connectivity During a Spatial Working Memory Task

by

Hailey Rosenblum

Approved: _____

Amy Griffin, Ph.D.
Professor in charge of thesis on behalf of the Advisory Committee

Approved: _____

Anna Klintsova, Ph.D.
Committee member from the Department of Psychological and Brain Sciences

Approved: _____

Jaclyn Schwarz, Ph.D.
Committee member from the Board of Senior Thesis Readers

Approved: _____

Michael Chajes, Ph.D.
Dean, University Honors College

ACKNOWLEDGMENTS

After taking my first neuroscience class during my first year at UD, I knew that the Department of Psychological and Brain Sciences was the perfect place for me to learn and explore my curiosity. Neuroscience utilized many of my interests such as biology, chemistry, and anatomy to discover the inner workings of the human brain, the most fascinating topic of all. Soon after I declared a major in neuroscience during my sophomore year, I began looking to join a lab and became interested in the learning and memory research in Dr. Amy Griffin's lab. Now, after nearly two years in the lab, I can say that it has been the most transformative learning experience of my time at UD. I would first like to thank Dr. Griffin for allowing me the opportunity to join the lab as an uncertain student with no previous research experience, and for supporting me throughout my involvement in undergraduate research. I would also like to thank SuHyeong Kim for being the best graduate student mentor anyone could ask for. She has supported me over the past two years both inside the lab and out, and I wouldn't be where I am today without her guidance. Additionally, I would like to thank John Stout for teaching me about data analysis and for being an amazing source of advice throughout my time in the lab. I would also like to thank Allison George for teaching me how to make electrophysiology components when I first joined the lab and for being helpful and patient with me throughout the learning process. Thank you Griffin Lab for being such an amazing learning environment, and I am so excited to continue my involvement next year through the 4+1 Master's Program in Neuroscience. Finally, I would like to thank my parents, my sister, and my friends for supporting and encouraging me throughout the last four years.

TABLE OF CONTENTS

LIST OF FIGURES

ABSTRACT

The brain growth spurt is a period of rapid brain growth and development which occurs during the third trimester of human pregnancy and the first two postnatal weeks in rodents. The hippocampus and medial prefrontal cortex (mPFC), structures which are important for spatial working memory, are vulnerable to alcohol exposure (AE) during the brain growth spurt. The nucleus reuniens (RE) of the thalamus has been demonstrated to play a role in orchestrating mPFC-hippocampus interactions which are necessary for spatial working memory. The RE has also been shown to be damaged due to AE in a third trimester rodent model. Recently, our lab has shown that rats exposed to alcohol during the brain growth spurt display spatial working memory impairments. The current study examines mPFC-hippocampus theta synchrony to determine if these effects can be explained by altered functional connectivity between these regions.

In this study we measured mPFC-hippocampus theta coherence, a metric that describes the degree to which mPFC-hippocampus theta rhythms are temporally correlated. We hypothesized that rats exposed to alcohol during the brain growth spurt would show reduced mPFC-hippocampus theta synchrony compared to sham intubated (SI) rats during decision making. Specifically, we predicted that AE rats would show reduced theta coherence at the choice point of a T-maze as they performed a spatial working memory task.

To study our hypothesis, pups were administered 5.25 g/kg/day alcohol via intragastric intubation between postnatal days 4-9. The sham intubated (SI) group received intubation without alcohol. Once rats reached adulthood (postnatal day 90), they completed pre-training in a T-maze to become familiarized with the testing environment. Rats then underwent local field potential (LFP) electrode implantation surgery, during which stainless steel wires were implanted into the mPFC and hippocampus. Once recovered from surgery, rats were trained on the

continuous alternation (CA) task, which is not a hippocampus dependent task but allowed rats to learn the alternation rule. Upon reaching the choice accuracy criterion of 80% for two consecutive days, rats learned the spatial working memory-dependent delayed alternation (DA) task. Each DA session consisted of 10 second, 30 second, and 60 second delay trials, with 12 trials of each delay length in a pseudorandom sequence. LFPs were recorded as rats performed the task. We then analyzed mPFC-hippocampus theta synchrony at the choice point of the T-maze.

In support of our hypothesis that AE during the brain growth spurt reduces mPFC-hippocampus theta synchrony, we found that DA task recording sessions of AE rats showed lower mPFC-hippocampus theta coherence when rats occupied the maze choice point compared to sessions of SI rats. Neural activity within brain regions was also altered, as hippocampus theta power was increased in sessions from AE rats compared to sessions from SI rats. These findings can help explain our previous finding of impaired spatial working memory in AE rodents. This study is important because it contributes to filling the gap in knowledge of how developmental AE affects cognitive function and the underlying mechanisms later in life.

Chapter 1

INTRODUCTION

1.1 Fetal Alcohol Spectrum Disorders

Fetal Alcohol Spectrum Disorders (FASDs) are a spectrum of disorders resulting from alcohol exposure (AE) *in utero* with an estimated prevalence of 1-5% among children in the United States and 1-10% globally (Hoyme et al., 2016; May et al., 2018). FASDs are the most common preventable neurodevelopmental disability in the world, and include fetal alcohol syndrome, partial fetal alcohol syndrome, alcohol-related neurodevelopmental disorder, and alcohol-related birth defects (de Sanctis et al., 2011; Hoyme et al., 2016; Williams et al., 2015). Severity and persistence of deficits caused by prenatal AE such as structural anomalies and neurobehavioral and cognitive impairments are impacted by timing and amount of exposure (de Sanctis et al., 2011; Hoyme et al., 2016; Williams et al., 2015). In addition to effects on health, FASD negatively impacts society in terms of human suffering, unrealized productivity, and economic burden (Hoyme et al., 2016). Animal models of FASD enable scientists to study AE during different periods of pregnancy to better understand the resulting effects on brain and behavior.

1.2 Alcohol Exposure during the Brain Growth Spurt

The third trimester of human pregnancy is characterized by processes such as neurogenesis, gliogenesis, differentiation and maturation, synaptogenesis, dendritic growth, and myelination (Coles, 1994; Dobbing & Sands, 1973; Ikonomidou et al., 2000; Milbocker et al., 2021; Roebuck et al., 1998; Semple et al., 2013). The brain growth spurt occurs during the third trimester of pregnancy in humans and the first two postnatal weeks in rodents (Coles, 1994;

Dobbing & Sands, 1979). It is a critical period for the development of the medial prefrontal cortex (mPFC) and hippocampus, and studies of animal models have demonstrated that AE during this time damages these regions (Bonthius & West, 1991; Hamilton et al., 2010, 2017; Ikonomidou et al., 2000; Lawrence et al., 2012; Livy et al., 2003; Murawski et al., 2012; Otero et al., 2012; Tran & Kelly, 2003; Whitcher & Klintsova, 2008; D. F. Wozniak et al., 2004). For example, studies have shown that the PFC undergoes apoptotic cell death and a reduction in dendritic spine density in pyramidal cells (Ikonomidou et al., 2000; Lawrence et al., 2012; Whitcher & Klintsova, 2008) and the hippocampus undergoes apoptotic cell death and a reduction in CA1 volume and pyramidal cell density and number (Bonthius & West, 1991; Livy et al., 2003; Murawski et al., 2012; Tran & Kelly, 2003; D. F. Wozniak et al., 2004).

In addition to structural effects, AE also alters functional connectivity (Candelaria-Cook et al., 2021; Little et al., 2018; Tang et al., 2018; Wilson et al., 2011; J. R. Wozniak et al., 2017), which is the interaction between different brain regions via the coordination of neural activity (Gordon, 2011). These changes have been related to impaired cognitive function (Little et al., 2018; Tang et al., 2018; Wilson et al., 2011; J. R. Wozniak et al., 2017). Executive functions, which are processes involved in goal-directed behaviors such as inhibition, set shifting, and working memory, are dependent on the prefrontal cortex (Rabinovici et al., 2015). Our 3rd trimester rodent model has previously shown altered neuroanatomical connectivity and impaired executive functioning (Gursky et al., 2021; Smith et al., 2022). Previous studies have additionally demonstrated that 3rd trimester AE impairs spatial working memory in mice (D. F. Wozniak et al., 2004) and rats (Girard et al., 2000; Thomas et al., 1996).

1.3 Spatial Working Memory

Spatial working memory describes the ability to maintain relevant spatial information over short time periods to perform goal-directed tasks. It is widely known that the mPFC, hippocampus, and their communication are important for spatial working memory in rodents (Churchwell & Kesner, 2011; Jones & Wilson, 2005; Maharjan et al., 2018; O'Neill et al., 2013; Spellman et al., 2015). In support of the importance of mPFC-hippocampus interactions for spatial working memory, Churchwell & Kesner, 2011 showed that communication between these structures is necessary when information is stored over long delay periods, whereas the mPFC and hippocampus can act independently over short delay periods.

The mechanisms that underlie mPFC-hippocampus interactions are not fully understood. Lesion studies have shown that the dorsal hippocampus, which receives visual, auditory and somatosensory information via connections to the entorhinal cortex, is involved in spatial learning and memory, while the ventral hippocampus, which has connections to the amygdala and hypothalamus, is involved in processes such as fear and anxiety (Bannerman et al., 2003, 2004; Hock & Bunsey, 1998; E. Moser et al., 1993; M.-B. Moser & Moser, 1998) The ventral hippocampus, but not the dorsal hippocampus, projects directly to the mPFC (Hoover & Vertes, 2007; Jay & Witter, 1991; Varela et al., 2014). There are also no known direct return projections from the mPFC to the hippocampus (Vertes et al., 2007).

The thalamic nucleus reuniens (RE) is reciprocally connected to both the mPFC and dorsal hippocampus, and recent research on mPFC-hippocampus connectivity has found that the RE plays a role in orchestrating mPFC-hippocampus communication (Cassel et al., 2013; Hallock et al., 2016; Layfield et al., 2015; Su & Bentivoglio, 1990; Varela et al., 2014; Vertes, 2002; Vertes et al., 2006, 2007). The Griffin lab has shown that pharmacological inactivation of

the RE impairs spatial working memory performance during a delayed alternation (DA) task and disrupts mPFC-hippocampus theta synchrony (Hallock et al., 2016; Layfield et al., 2015). Previously, the Klintsova Lab found a reduction in neuron number and volume in the RE in our 3rd trimester rodent model (Gursky et al., 2019, 2020; Smith et al., 2022), showing that the RE is vulnerable to AE during this period of development.

AE during the brain growth spurt damages the hippocampus, mPFC, and RE, which could result in altered functional connectivity between these brain regions. Recently, we found that our 3rd trimester binge rodent model of FASD displays impairments in spatial working memory compared to sham intubated (SI) controls (Kim et al., 2021). It is possible that these spatial working memory deficits are related to changes in functional connectivity in mPFC-RE-hippocampus circuitry.

1.4 Recording Local Field Potentials (LFPs) from the Hippocampus and mPFC

One way to examine functional connectivity is through recording local field potentials (LFPs) to determine the extent to which neural activity between regions is synchronized (Gordon, 2011). LFPs are the electrical potentials of a population of neurons and are measured by inserting electrodes into the region of interest (Sharott, 2014). Membrane potential fluctuations result in LFP oscillations. Coherence is used as a measure of oscillatory synchrony between brain regions, showing how coordinated two signals are to each other (Gordon, 2011).

It has been shown that theta oscillations (4-12 Hz) are important for mPFC-hippocampus synchronization during spatial working memory tasks (Hallock et al., 2016; Hyman et al., 2010; Jones & Wilson, 2005; O'Neill et al., 2013; Sigurdsson et al., 2010). Jones & Wilson, 2005 examined mPFC-hippocampus LFP theta coherence as rats performed a spatial working memory task. During forced-turn epochs of the task, rats were forced to turn either right or left

irrespective of previous maze location. During choice epochs, which were spatial working memory-dependent, rats had to turn in the opposite direction as the forced-turn epoch to receive a reward. Jones & Wilson, 2005 demonstrated that mPFC-hippocampus LFP theta coherence was increased during correct trials of choice epochs of the task compared to forced-turn epochs. It was additionally found that theta coherence was reduced during incorrect trials of choice epochs compared to correct choice epochs. A study by O'Neill et al., 2013 showed that mPFC and ventral hippocampus theta oscillation amplitude in mice was highest during choice phases of a discrete non-match to sample test in a T-maze, during which previous experiences must be assessed to make a decision. During the sample phase, mice were directed from the center arm into a goal arm of the T-maze. During the choice phase, which took place after a delay, mice ran back down the center arm and had to choose the opposite goal arm as the sample phase to receive a reward. It was shown that theta coherence between the mPFC and dorsal hippocampus increased during choice phases compared to sample phases. Taken together, these results demonstrate that mPFC-hippocampus theta synchrony is increased when spatial working memory demand is present and that theta oscillations are involved in decision making.

1.5 Hypothesis and Prediction

The current study further investigates previous findings of our lab by examining the effects of 3rd trimester binge AE on mPFC-hippocampus theta synchrony during a spatial working memory task. Specifically, we examined synchrony at the choice point of a T-maze during the DA task. We hypothesized that AE during brain growth spurt would reduce mPFC-hippocampus theta synchrony during decision making during the DA task and predicted that the AE group would show reduced theta coherence compared to the SI group at the choice point of the maze.

Chapter 2

METHODS

2.1 Animal Subjects

Subjects were Long Evans hooded rats **(**AE females, n= 1; SI females, n= 1; AE males, n= 3; SI males, n= 5). The colony room was temperature and humidity controlled and followed a 12 hour light/dark cycle from 7am-7pm. Rats were given *ad libitum* access to food and water until the completion of handling, upon which they were placed on mild food restriction to maintain 90% of their *ad libitum* body weight. All animal procedures were performed in accordance with the University of Delaware Institutional Animal Care and Use Committee and the NIH Guide for the Care and Use of Laboratory Animals.

2.2 Animal Generation and Postnatal Treatment

On postnatal day 3, rats were paw marked for identification via injection of India black ink. Pups were then randomly assigned to either the AE group or sham intubated (SI) control group. AE group pups were administered 5.25 g/kg/day alcohol in a milk formula via intragastric intubation twice per day (separated by 2 hours: at approximately 9 a.m. and 11 a.m.) from postnatal days 4-9. During this same period, SI group pups received intubation but without any liquid in order to control for stress effects of intubation. Additionally, 2 hours (and 4 hours on postnatal day 4 only) after the second intubation on postnatal days 4-9 AE rats received a supplemental milk formula dose to prevent weight loss. After intubation on postnatal day 9, pups were ear punched for identification. Rats were housed with their dams until postnatal day 23, when they were weaned and housed in cages of 2-3 with the same sex.

2.3 Behavior Apparatus and Testing Room

Rats performed tasks in a wooden T-maze which was painted black and included a central arm (116 cm x 10 cm), two goal arms (56.5 cm x 10 cm), and two return arms (112 cm x 10 cm) with 6 cm high wooden walls. The reward (chocolate sprinkles) was placed in a small plastic cup at the end of each goal arm. Between forced run trials and DA task trials, rats waited in a start box (a barstool with a dish attached on top) blocked off from the stem of the maze by a removable wooden barrier (25 cm tall). The testing room was surrounded by a black curtain with attached visual cues of different shapes and colors. The room was dimly lit by 2 compact fluorescent bulbs.

2.4 Behavioral Training

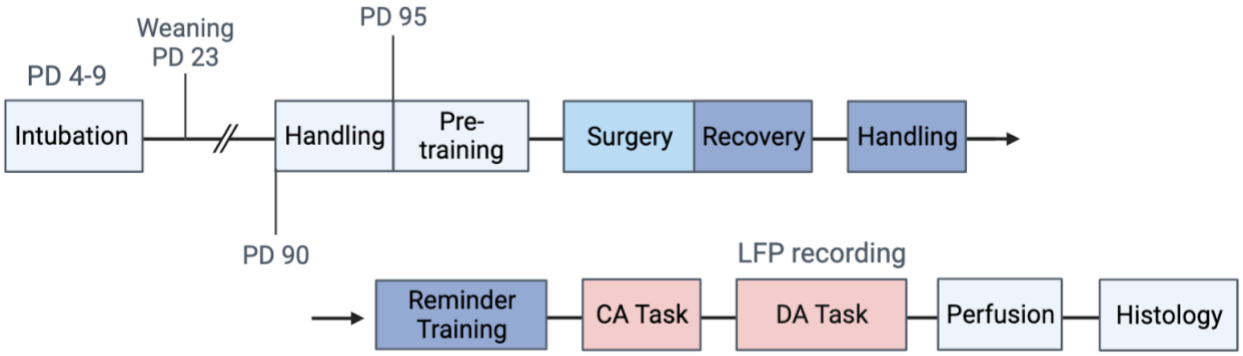

Figure 1. Experimental Timeline. PD = postnatal day, CA = continuous alternation, DA = delayed alternation. Created with BioRender.com

2.4.1 Handling and Pre-Training

When rats reached postnatal day 90, they were separated into single cages to begin mild food restriction. This step was necessary to ensure that rats would be motivated to consume the

food reward during memory task training. Experimenters then began to handle rats 10 minutes per day for 5 days. After each handling session, rats received a handful of sprinkles in the corner of their cage to familiarize themselves with the food reward of the memory tasks. After handling was completed, rats began pre-training to become acclimated to the testing environment.

First, rats completed goal-box training to become familiar with the reward zone of the T-maze. During training, the two goal arms of the maze were blocked off on both sides by two wooden barriers (25 cm tall). Chocolate sprinkles were placed in a small cup at the end of each goal arm. In a single trial, a rat was placed in one of the goal arms with the task of eating all the sprinkles in under 90 seconds. Once the rat ate all of the reward, or after a maximum of 3 minutes in a particular goal arm, they were transferred to the other goal arm to repeat the task. This procedure was repeated for a total of 6 trials per day (alternating between left and right goal arms). In order to move to the next stage of pre-training, forced run training, rats were required to finish the reward within 90 seconds during all 6 trials for 2 consecutive days.

The goal of forced run training is to familiarize rats with the route of the maze. During training, rats began the task in the start box at the base of the T-maze. Once the start box was opened, rats traveled down the central arm of the maze to the T-intersection. One of the goal arms of the T-maze was blocked off by a wooden barrier, which forced the rat to go in the direction of the other goal arm. Rats then traveled down the open goal arm, ate the food reward in the goal zone, and returned to the start box via the return arm. Rats remained in the start box while the experimenter set up for the next trial. One forced run session consisted of 12 left and right trials (6 of each in a pseudorandom sequence) (Fellows, 1967). Once the rats were qualified, they underwent local field potential (LFP) electrode implantation surgery.

2.4.2 Surgical Procedures

Rats were anesthetized with isoflurane (1.0-3.0% in oxygen) and were injected with atropine (0.06 mg/mL). Eye ointment was applied to the eyes before the rat's head was shaved around the incision site and was reapplied periodically throughout surgery. Once the rat no longer displayed the pedal reflex, they were placed into a stereotaxic instrument (Kopf). Once ear bars were in place, the incision site was sterilized with chlorhexidine solution and subcutaneously injected with lidocaine. Once the incision was made, hydrogen peroxide was applied to control bleeding. The head was then leveled and bregma was identified. The coordinates of the mPFC, dorsal hippocampus, and cerebellum drill sites were then calculated relative to bregma and a stereotaxically mounted drill was used to drill holes at these coordinates. The craniotomy above the mPFC was 3.1 mm anterior and 1.0 mm lateral to bregma. The craniotomy above the dorsal hippocampus was 3.7 mm posterior and 2.2 mm lateral to bregma on the ipsilateral hemisphere as the mPFC drill site. The cerebellum reference drill hole was 12 mm posterior and 2.2 mm lateral to bregma on the contralateral hemisphere as the mPFC and dorsal hippocampus drill sites. 4 small bone screws *(*Fine Science Tools) were then screwed into the skull (2 on each side of the skull) to stabilize the LFP bundles once implanted. A ground screw (a bone screw with stainless steel wire soldered to it) was screwed lateral to the cerebellum reference drill site. The mPFC wire bundle (containing 2 stainless steel wires of equal lengths) was then implanted 2.6 mm ventrally at an 8 degree angle at the previously mentioned mPFC coordinate and stabilized to the skull using adhesive cement (C&B Metabond). The hippocampus bundle (4 staggered stainless steel wires with 1 mm between the most ventral and dorsal wires), was then implanted 2.5 mm ventrally at the previously mentioned dorsal hippocampus coordinates and stabilized. Next, cerebellum reference wires (2 stainless steel wires twisted

together) were implanted 1mm ventrally at the previously mentioned coordinates and stabilized. Once all bundles were implanted, acrylic was used to secure a rod attached to the electrode interface board (EIB) to the skull. A copper mesh cage was fitted to surround the EIB and LFP wires and was secured to the skull using acrylic. The ground wire was then linked to the EIB via a connecting wire, which was then soldered to the copper mesh cage. All LFP wires were linked to the EIB with gold pins, and any exposed wire was covered with liquid electrical tape. Once the copper mesh cage was secure and all wires were attached, rats were injected with flunixin (Banamine; 50 mg/mL). To protect drive components, the EIB was covered by a small weigh boat which was velcroed to the copper mesh cage, and the copper mesh cage was wrapped with self adhesive bandage. A schematic of LFP drive components is shown in Figure 2. 25 mL of child ibuprofen (100 mg/5 mL) was added to drinking water in the home cage. After the completion of surgery, rats completed a minimum of 7 recovery days before beginning reminder training. All surgical procedures were approved by the University of Delaware Institutional Animal Care and Use Committee.

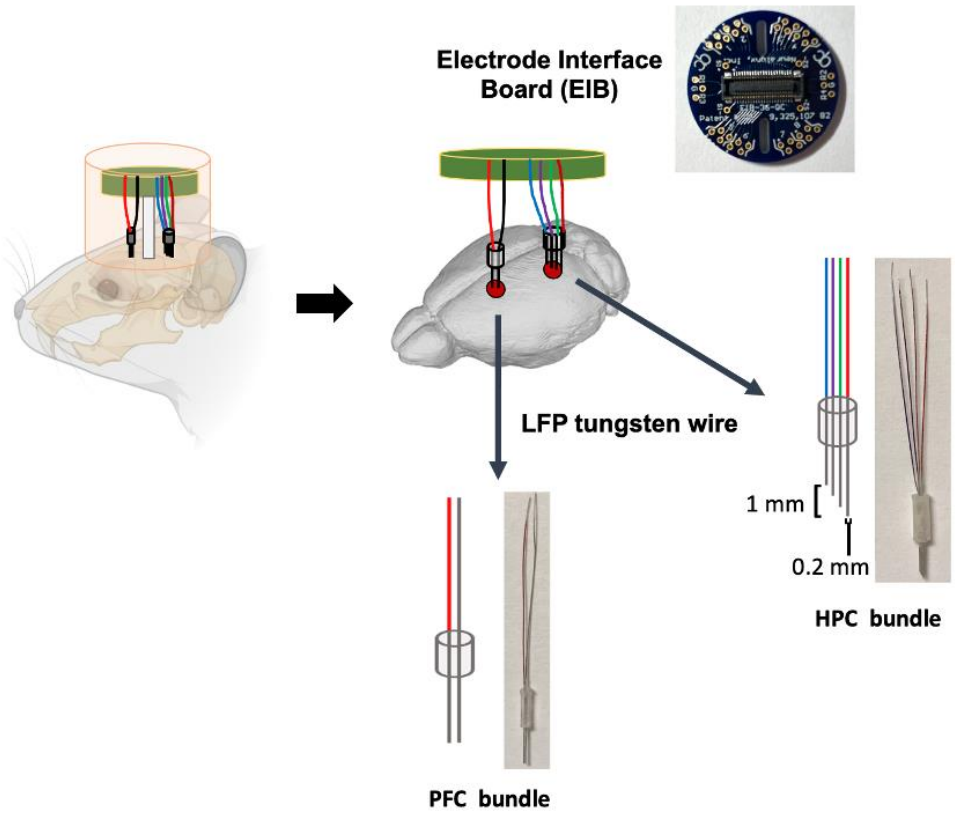

Figure 2. Local Field Potential Drive Components. LFPs were recorded by implanting stainless steel wires in the mPFC and dorsal hippocampus. 2 wires (wire diameter= 0.2 mm) were implanted into the mPFC and 4 wires (staggered, with 1 mm between the most dorsal and ventral wires) were implanted into the hippocampus (HPC). Wires were attached to the EIB, which was plugged into a headstage which sent recording data to the computer during DA task performance. The drive was attached to the skull and surrounded by a copper mesh cage to reduce noise during recording.

2.4.3 Continuous Alternation Task

After rats recovered from surgery and completed reminder pre-training they were trained on the continuous alternation (CA) version of the spatial alternation task which taught them the spatial alternation rule. During the CA task, rats continuously alternated between the left and right goal arms of the T-maze in a figure-eight pattern without returning to the start box (Figure 3). If a rat successfully alternated goal arms during a trial, they were rewarded with sprinkles in the goal zone. During each CA session, rats completed 40 trials, and in order to complete the

task, rats had to reach 80% choice accuracy for 2 consecutive days. The CA task is not hippocampus dependent and does not require spatial working memory demand (Ainge et al., 2007). As a result, rats were trained on this task before the DA task to determine if there were deficits when learning the alternation rule in AE rats compared to SI controls.

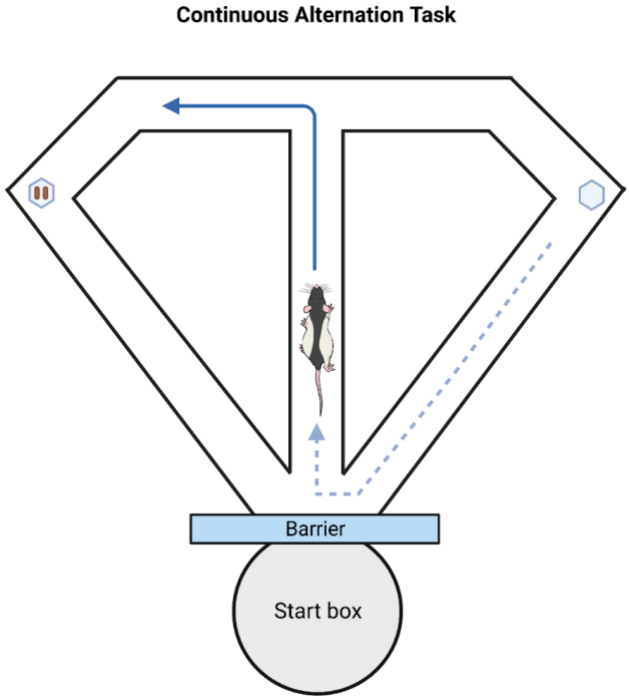

Figure 3. Continuous Alternation (CA) Task Schematic. Rats continuously alternated between goal zones of the T-maze to receive a reward. Created with BioRender.com.

2.4.4 Delayed Alternation Task and Electrophysiology Recording

After reaching criterion on the CA task, rats were trained on the DA task. Unlike the CA task, the DA task is hippocampus dependent (Ainge et al., 2007). During the DA task, rats alternated between goal arms of the T-maze, but a delay was inserted in between each alternation trial when rats returned to the start box (Figure 4). A total of 3 delay lengths (10 seconds (s), 30 s and 60 s; 12 rounds of each delay length) were introduced in between each trial in a

pseudorandom sequence. Cheetah software (Neuralynx) was used to record LFP data from the mPFC and dorsal hippocampus as rats performed the DA task.

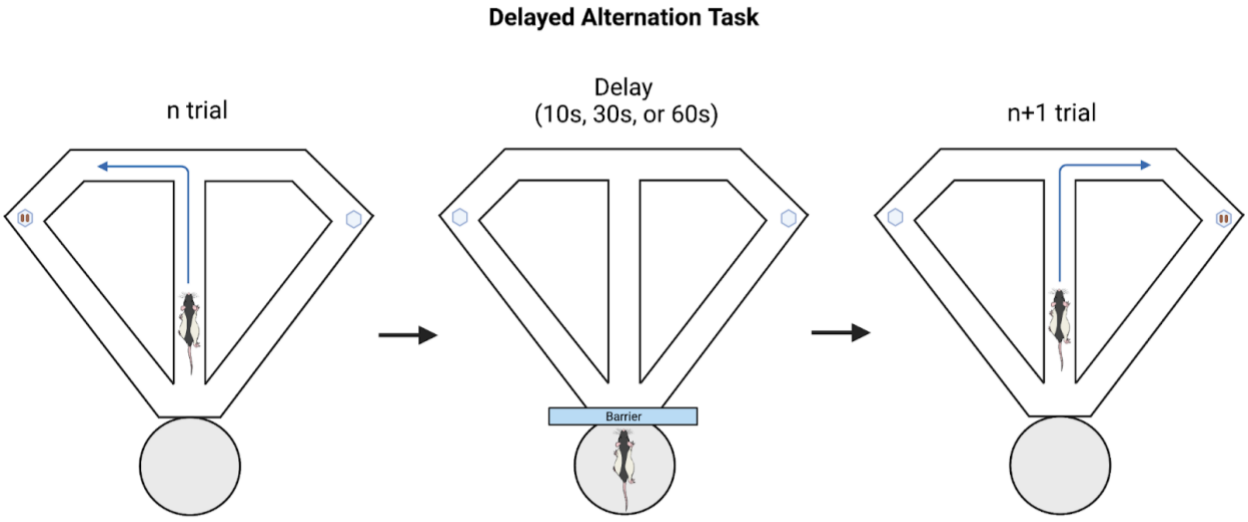

Figure 4. Delayed Alternation (DA) Task Schematic. In addition to following the alternation rule learned in the CA task, rats returned to the start box between trials for either 10 seconds (s), 30 s, or 60 s. Created with BioRender.com.

2.4.5 Perfusion and Histology

After completion of DA task recording, rats were anesthetized with isoflurane and administered a veterinarian-approved mixture of xylazine and ketamine intraperitoneally. Once rats no longer displayed the pedal reflex, they were perfused transcardially with 100 mL of heparinized 0.1 M phosphate buffered saline (PBS) (pH = 7.20) and 100 mL of 4% paraformaldehyde in 0.1M PBS (pH = 7.20). Next, the head was postfixed in 4% paraformaldehyde solution for 48 hours, upon which time the brain was extracted and transferred through three solutions of 30% sucrose in 4% paraformaldehyde (24-72 hours in each solution based on the time needed for the brain to sink to the bottom of the solution). This has been shown to be an important cryoprotecting process in preventing freezing artifacts during

sectioning with a cryostat (Rosene et al., 1986). The brain was then stored at 4°C until cryosectioning. Once postfixing was completed, a Leica cryostat (20°C) was used to generate 40 µm coronal sections of the brain, which were then stored chronologically in a sucrose/ethylene glycol cryoprotectant solution at 20°C until electrode placement verification. Electrode placement is verified by superimposing an image of the coronal section on a plate from the stereotaxic atlas (Figure 5).

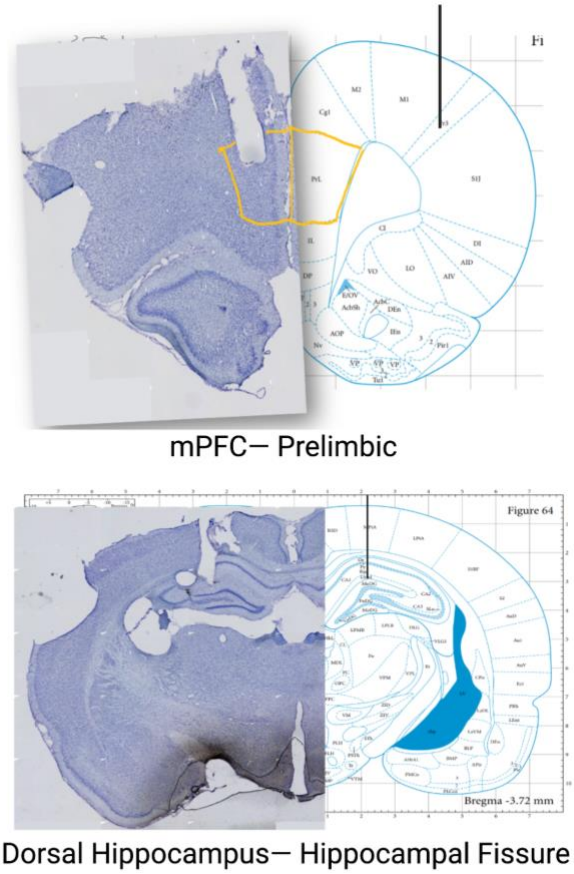

Figure 5. Example of electrode placement verification. mPFC (top) and dorsal hippocampus (bottom) wire placement is checked by superimposing an image of the brain section (left) on a plate from the stereotaxic atlas (right). In the top image, the mPFC wire was implanted within the prelimbic region of the mPFC, which is outlined in yellow. In the bottom image, the dorsal hippocampus wire was implanted into the hippocampal fissure, as compared to the black line shown in the plate from the stereotaxic atlas.

2.5 mPFC-Hippocampus Coherence

Position data was recorded as rats performed the DA task. LFPs from the mPFC and hippocampus were extracted at the choice point of the T-maze, which is the area around the T-intersection where rats made a decision to turn left or right (Figure 7A). To receive a reward, rats had to alternate between trials. The coherence analysis consisted of mPFC and hippocampus LFP recordings from 0.5 seconds before rats reached the choice point entry until 1 second after rats reached the choice point entry during task performance (Figure 6A), which tended to capture as rats approached the choice point and engaged in choice-behaviors (Figure 6B). The analysis controlled for time, focusing on 1.5 second time windows, based on currently unpublished data from our lab finding that about 1.25 seconds of data is sufficient for reliable estimates of theta coherence. The choice point entry was chosen based on divergence in trajectory at the choice-point. Magnitude-squared coherence (*mscohere.m*) was used in MATLAB to measure coherence between mPFC and hippocampus oscillations recorded at the choice point of the maze during the task.

$$C_{xy}(f) = \frac{\left|P_{xy}(f)\right|^2}{P_{xx}(f)P_{yy}(f)}$$

The function utilizes the power spectral density of signals x and y, $P_{xx}(f)$ and $P_{yy}(f)$, and the cross power spectral density $P_{xy}(f)$ to determine a coherence value. Power spectral density measures the power of a signal over a range of frequencies, and the cross power spectral density uses the cross-correlation of two signals to determine the power distribution per given frequency. Coherence was measured over a frequency range of 1-20 Hz at a frequency resolution of 0.5 Hz. Coherence values range between 0, meaning that the signals are not coherent and are not correlated with each other, and 1, meaning that the signals are perfectly coherent.

2.6 mPFC and Hippocampus Power Spectra

Power spectral density was calculated using a multitaper method with 3 multitapers and a time-bandwidth product of 2 (Mitra, 2007; *mtspectrumc.m*). LFPs were extracted from the mPFC and hippocampus at the choice point using the same method as described above for the coherence analysis.

2.7 Statistical Analysis

The Rank-sum test was performed in MATLAB to test the significance of mPFC-hippocampus theta coherence (Chapter 3.1), time spent in the choice point (Chapter 3.2), and mPFC and hippocampus theta power (Chapter 3.3) between DA task sessions performed by AE and SI rats.

Chapter 3

RESULTS

3.1 Significantly Reduced Theta Coherence at Choice Point in AE Rat Sessions

To determine if theta coherence is altered during decision making in AE rats, LFP recordings were analyzed from 0.5 seconds before until 1 second after rats entered the choice point entry (Figure 6A). The positions of AE and SI rats within this time window are shown in Figure 6B. The median position for LFP analysis is consistent across sessions performed by AE and SI rats, showing that analysis for both groups included data from rats approaching the choice point and engaging in decision making.

mPFC-hippocampus coherence was calculated for DA task sessions of AE and SI rats (AE: N = 59 sessions, SI: N = 86 sessions). The distribution of coherence values as a function of frequency in sessions performed by AE and SI rats is shown in Figure 6C. Theta coherence was highest within the 6-9 Hz range for sessions from both AE and SI rats. AE rats displayed significantly lower theta coherence (6-9 Hz) across sessions of the DA task compared to SI controls ($Z = -3.9$, $p < 0.001$, Rank-sum test; Figure 6D).

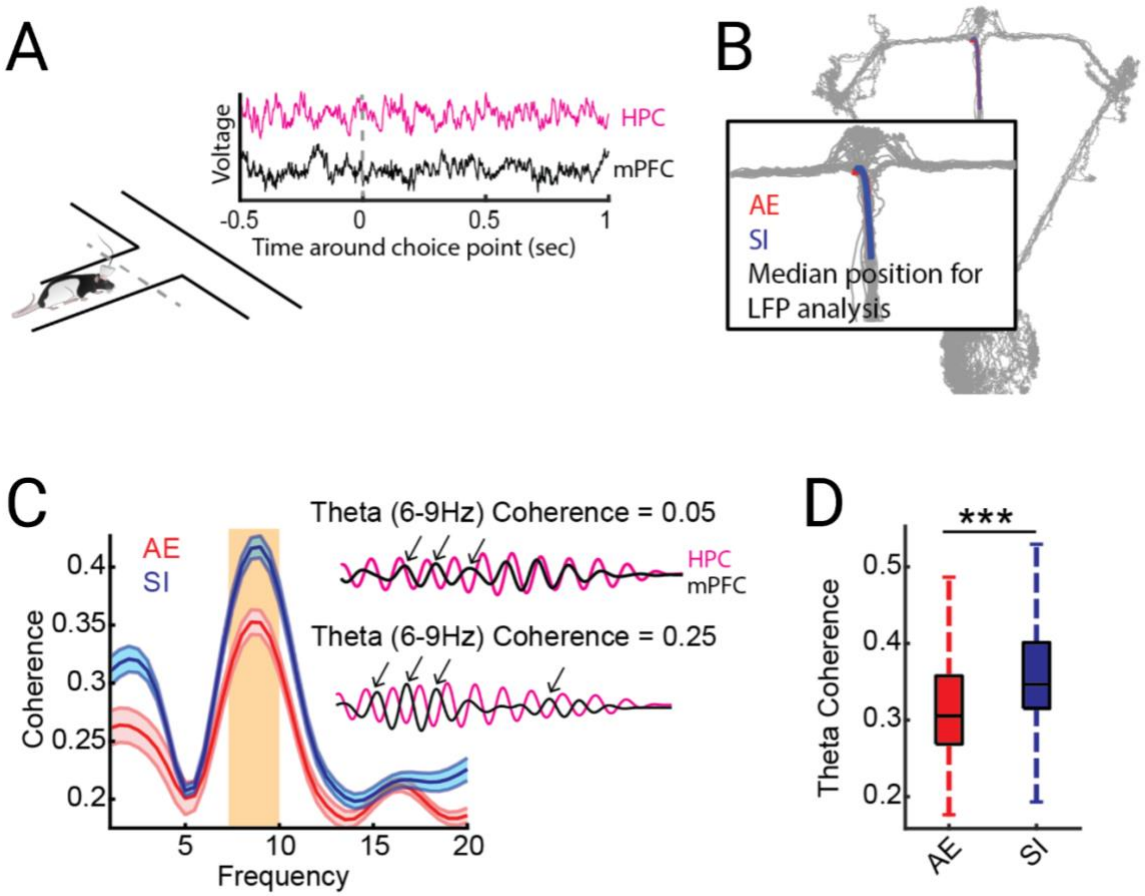

Figure 6. DA task recording sessions of AE rats show reduced mPFC-hippocampus (HPC) theta coherence during decision making compared to sessions of SI rats. **(A)** mPFC and hippocampus LFPs recorded from –0.5 seconds to +1 second relative to choice point entry (dashed line) were utilized in analysis. **(B)** Median position for LFP analysis of AE (red) and SI (blue) rats between –0.5 seconds to +1 second relative to choice point entry. **(C)** Distribution of coherence values as a function of frequency from sessions performed by AE and SI rats during decision making. Frequencies between 6-9 Hz are highlighted; subsequent analyses occur within this frequency range. Subpanels show examples of filtered signals with corresponding low (top) and high (bottom) theta coherence values. Signals with high coherence show higher phase consistency compared to signals with low coherence (reference arrows at mPFC peaks to phase of hippocampus theta signal). **(D)** Theta coherence is reduced in AE rats' sessions compared to SI rats' sessions ($Z = -3.9$, $p < 0.001$; Rank-sum test). ***$p < 0.001$.

3.2 AE and SI Rats Show No Significant Difference in Time Spent at Choice Point

We wanted to determine if postnatal AE affected the amount of time rats spent at the choice point of the T-maze before making a decision to turn left or right during the DA task. Differences in the amount of time spent could indicate altered choice-behaviors after AE during the brain growth spurt. The choice point was defined as a boxed area around the T-intersection of the maze (Figure 7A). There was no significant difference in the amount of time spent in the choice point between DA sessions of AE and SI rats ($Z = -0.63$, $p = 0.53$, Rank-sum test; Figure 7B).

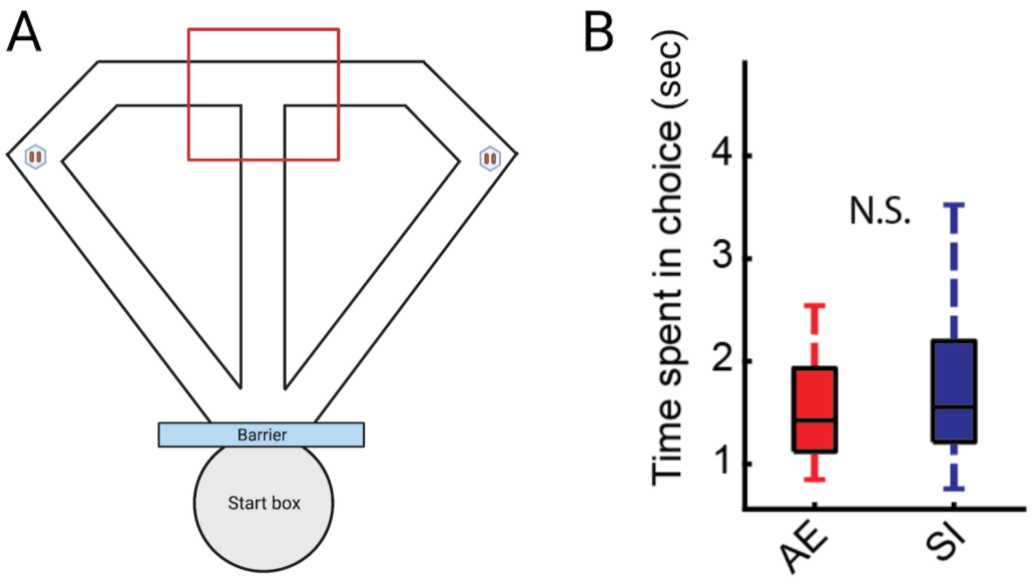

Figure 7. Time spent in the choice point. **(A).** Maze schematic with choice point represented as a red box at the T-intersection. **(B).** AE and SI rats did not show a significant difference in the amount of time spent at the choice point during sessions of the DA task ($Z = -0.63$, $p = 0.53$; Rank-sum test).

3.3 Increased Hippocampus Theta Power in Recording Sessions of AE Rats

The distribution of power as a function of frequency for sessions performed by AE and SI rats is shown in Figure 8A. While there was no significant difference in mPFC theta power (6-9 Hz) during choice point occupancy between recording sessions of AE and SI rats ($Z = -1.3$, $p = 0.18$; Rank-sum test; Figure 8B), sessions of AE rats had significantly higher hippocampus theta power compared to sessions of SI rats ($Z = 2.7$, $p < 0.01$; Rank-sum test; Figure 8B).

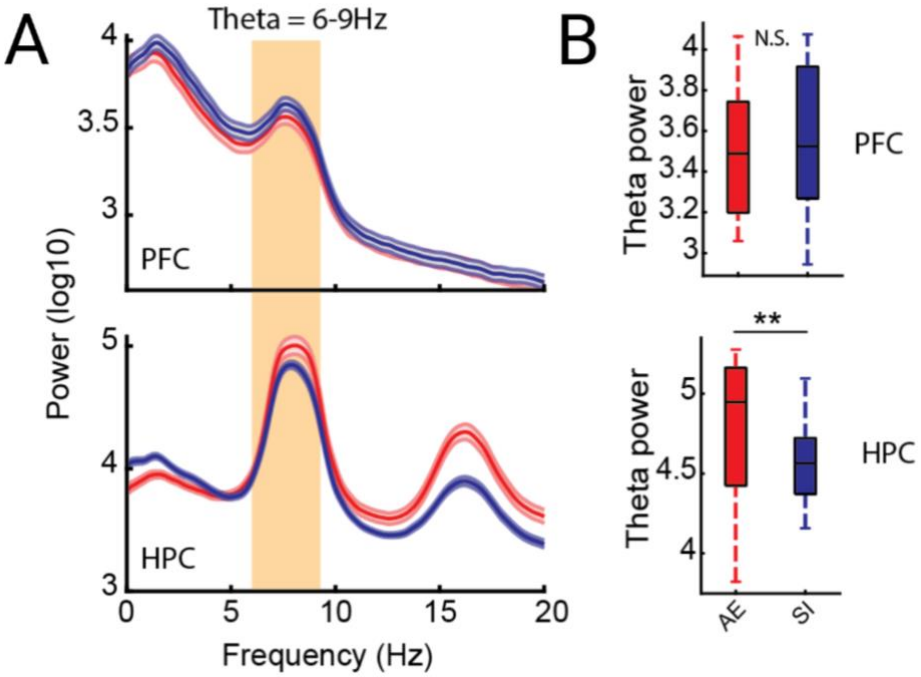

Figure 8. DA sessions of AE rats show stronger hippocampal theta power and similar mPFC theta power compared to SI controls. **(A)** The distribution of power as a function of frequency for mPFC (top) and hippocampus (bottom) LFPs at the choice point during the DA task. Frequencies between 6-9 Hz are highlighted. **(B)** Top: mPFC theta power is not significantly different between sessions of AE and SI rats ($Z = -1.3$, $p = 0.18$; Rank-sum test). Bottom: Hippocampus theta power is significantly increased in sessions performed by AE rats compared to SI rats ($Z = 2.7$, $p < 0.01$; Rank-sum test). **$p < 0.01$.

Chapter 4

DISCUSSION

4.1 Summary

In this study, we demonstrated that recording sessions of AE rats showed reduced hippocampal-mPFC theta coherence compared to sessions of SI rats during decision making in a spatial working memory task. For the current study, rats were either exposed to alcohol between postnatal days 4-9 via intragastric intubation (AE group) or were intubated without exposure to alcohol (SI group). Once rats reached adulthood at postnatal day 90, they were trained to complete the DA task to examine the effects of AE during the brain growth spurt on mPFC-hippocampus functional connectivity during decision making, specifically through examining mPFC-hippocampus theta coherence at the choice point of a T-maze as they performed the task. At the choice point of the maze, rats had to recall the previous choice outcome to guide their subsequent decision to turn left or right. Our hypothesis was confirmed, as AE reduced mPFC-hippocampus theta synchrony at the choice point during the DA task. In support of our prediction, AE rats' sessions of the DA task showed significantly lower theta coherence (6-9 Hz) compared to SI rats' sessions at the choice point of the T-maze. As there was no significant difference in time spent at the choice point and experimenters were blind to group, these findings suggest that AE rats have decreased mPFC-hippocampus theta synchrony. While previous studies have shown adult rats exposed to alcohol during the brain growth spurt experience structural damage and spatial working memory deficits, these are the first results to indicate that AE during this period of development alters mPFC-hippocampus interactions.

4.2 Effects of 3rd Trimester AE on mPFC-RE-Hippocampus Circuitry

Changes in mPFC-hippocampus theta synchrony in our third trimester rodent model could be due to alcohol-induced structural damage during the brain growth spurt, an important period for brain development, to areas such as the mPFC, hippocampus, and RE. Previously, it has been shown that the hippocampus is vulnerable to AE during the third trimester equivalent, resulting in a reduction in pyramidal cell number and density in the hippocampal CA1 and CA3 regions and a reduction in granule cell number and density in the dentate gyrus (Bonthius & West, 1991; Livy et al., 2003; Murawski et al., 2012; Wilson et al., 2011). The PFC is also vulnerable to AE in rodent models of the brain growth spurt, as shown through apoptotic cell death after exposure and reduced dendritic spine density in pyramidal cells (Ikonomidou et al., 2000; Lawrence et al., 2012; Whitcher & Klintsova, 2008). The RE, which is important for coordinating mPFC-hippocampus communication (Cassel et al., 2013; Hallock et al., 2016; Layfield et al., 2015; Su & Bentivoglio, 1990; Varela et al., 2014; Vertes, 2002; Vertes et al., 2006, 2007), has been shown to undergo neuronal apoptosis and a reduction in volume in a 3rd trimester binge AE rodent model (Gursky et al., 2019, 2020; Smith et al., 2022)

4.3 The mPFC, RE, and Hippocampus in Spatial Working Memory

Various studies have shown the participation of and interaction between the mPFC and hippocampus are important for spatial working memory (Churchwell & Kesner, 2011; Lee & Kesner, 2003; Maharjan et al., 2018; Wang & Cai, 2006). Churchwell & Kesner, 2011 examined spatial working memory performance after inactivating the mPFC and intermediate CA1 (iCA1) region of the hippocampus during a delayed non-match to place task on a radial 8-arm maze. During the task, rats first completed a study phase, during which one arm of the maze was open and contained the reward. After receiving the reward and returning to the center platform, rats

waited for either a short (10 seconds) or long (5 minutes) delay before the test phase, during which two arms were open and the reward was located in the non-match arm. Researchers compared the effects of contralateral inactivation, which resulted in the disconnection of mPFC and iCA1 interactions in the brain, and ipsilateral inactivation, which kept mPFC-hippocampus interactions intact in one hemisphere of the brain, to saline controls of each condition. Churchwell & Kesner, 2011 found that contralateral inactivation of the mPFC and iCA1 via muscimol infusion increased errors during 5 minute delay trials compared to ipsilateral inactivation during the 5 minute delay, showing that interactions between these regions are necessary for spatial working memory. In contrast, this effect was not seen after the 10 second delay (low working memory demand condition), showing that the iCA1 and mPFC can process spatial working memory information independently when demand is low.

Communication between the mPFC and hippocampus via theta synchronization is important for spatial working memory (Hallock et al., 2016; Hyman et al., 2010; Jones & Wilson, 2005; O'Neill et al., 2013; Sigurdsson et al., 2010). In a study by Hallock et al., 2016, rats were trained on both the DA task, with 30 second delays between trials, and a spatial working memory-independent conditional discrimination task (CD), a mPFC and dorsal hippocampus independent task (Hallock et al., 2013; Shaw et al., 2013) during which decisions were based on the texture and color of floor inserts in the maze. In sessions containing both good CD and DA task performance, theta coherence at the choice point was higher during the DA task compared to CD task. These results demonstrate that tasks with spatial working memory demand (e.g. DA task) show stronger mPFC-hippocampus interactions compared to tasks without this demand (e.g. CD task).

Inactivation of RE additionally impairs spatial working memory ability and disrupts mPFC-hippocampus theta synchrony (Hallock et al., 2016; Layfield et al., 2015). Layfield et al., 2015 showed that pharmacological inactivation of the RE and rhomboid nucleus (Rh) resulted in impaired spatial working memory performance on the DA task with either 5 second delays or 30 second delays, but not on the CA task. The insertion of delays between DA trials makes this a spatial working memory dependent task, and thus dependent mPFC-hippocampus interactions. As a result, impaired DA task performance after RE inactivation indicates that the RE is an important modulator of mPFC-hippocampus interactions. Hallock and colleagues (2016) pharmacologically inactivated the RE/Rh with muscimol and recorded mPFC and hippocampus LFPs as rats performed the DA task. DA task performance was significantly lower after muscimol infusion compared to task performance at baseline. In addition, when mPFC-hippocampus theta coherence was analyzed at the choice point during muscimol conditions, it was significantly lower compared to theta coherence at baseline. Taken together these findings demonstrate the role of the RE in mediating mPFC-hippocampus interactions.

4.4 Increased Hippocampal Theta Power in Sessions Performed by AE Rats

In addition to reduced theta coherence between the mPFC and hippocampus in AE rats' recording sessions compared to SI rats' sessions, hippocampal theta power was increased in sessions recorded from AE rats. While previous studies have shown that theta power is influenced by acceleration (Long et al., 2014) and speed (Hinman et al., 2011; McFarland et al., 1975; Whishaw & Vanderwolf, 1973), we did not find differences in time spent at the choice point between DA task sessions performed by AE and SI rats. As time spent is an indirect measurement of speed, it is unlikely that changes in speed drove this increase in hippocampal theta power in AE rats' sessions. However, we will investigate acceleration in our future analysis

to determine if there is a correlation between acceleration and increased hippocampal theta power. This effect could also be due to recording electrodes being located along differing hippocampal lamina among AE and SI rats. Theta amplitude is different depending on depth in the hippocampus, with the highest power recorded near the hippocampal fissure (Bragin et al., 1995; Buzsáki, 2002; Buzsáki et al., 1985, 1986). It is possible that theta power would be different if recording electrodes between groups are located at different depths. As electrode placement verification is in progress, we are currently unable to make a conclusion on the cause of this finding. An additional explanation for our finding of increased hippocampal theta power in sessions performed by AE rats could be that AE altered hippocampal excitability, as there has been a previous finding of hippocampal hyperexcitability in a rodent model of FASD (Krawczyk et al., 2016).

Future analyses will also examine power at other frequency ranges. Our current results appear to show an increase in hippocampal power in sessions from both AE and SI rats around 16 Hz, with the greatest increase seen in AE rats. It is likely that this increase in hippocampal power is a harmonic of theta unrelated to beta rhythms (15-30 Hz). A study by Sheremet and colleagues (2016) examined the nonlinearity of theta rhythms in the dorsal hippocampus in relation to running speed. Researchers found that theta rhythm nonlinearity increased as rat speed increased, as shown by a chain of harmonics which were coupled to theta oscillations, with the second harmonic of theta occurring at 16 Hz. In future analyses, we will analyze velocity during the DA task, which could help explain this increase in hippocampal power. Another possibility for increased power in the beta frequency range could be explained by a recent study by Jayachandran et al., 2022 which found that beta bursts in mPFC-RE-hippocampus circuitry play a role in episodic memory. Researchers first investigated mPFC-hippocampus LFPs as rats

performed a nonspatial sequency memory task. Jayachandran and colleagues found that beta power and coherence were greatest during memory trials of the task, when rats were tested on their memory of an odor sequence, while theta power and coherence were greatest during running periods of the task. They additionally found that beta bursts occurred in the RE shortly before these bursts occurred in the hippocampus, demonstrating a role for the RE in driving mPFC-hippocampus beta synchrony.

Overall, in the context of the current findings it is unlikely that the increase in hippocampal theta power is driving the decrease in mPFC-hippocampus coherence in sessions from AE rats. If this were the case, the greater increase in hippocampal power in the 15-20 Hz range in AE rats' sessions would have been paired with reduced coherence compared to SI rats' sessions at this frequency range.

4.5 Relating Findings to Previous Studies

While no studies to our knowledge have investigated functional connectivity between the mPFC and hippocampus in a 3rd trimester AE rodent model, previous studies have shown that AE during pregnancy alters neural activity within, and functional connectivity between brain regions (Candelaria-Cook et al., 2021; Tang et al., 2018; Wilson et al., 2011; J. R. Wozniak et al., 2017). Our finding of increased hippocampal theta power in recording sessions from AE rats is consistent with a previous study by Wilson et al., 2011. Wilson and colleagues (2011) studied a mouse model of 3rd trimester binge drinking that showed changes in circuit function into adulthood. It was found that odor evoked theta-band LFP activity was increased in the hippocampus, olfactory bulb (OB), and anterior piriform cortex (aPCX) in AE mice. When researchers examined functional connectivity in the olfacto-hippocampal pathway using spontaneous LFPs from these regions, ethanol-treated mice showed increased coherence between

the OB and aPCX in the beta and delta frequency ranges and increased coherence between aPCX and dorsal hippocampus in the beta frequency range.

Other disorders which are characterized by working memory deficits, such as schizophrenia, have also shown altered functional connectivity between the hippocampus and prefrontal cortex. A study by Sigurdsson et al., 2010 examined firing of mPFC cells in relation to the phase of hippocampal theta oscillations and theta coherence of mPFC-hippocampus LFPs during a discrete non-match-to-sample spatial working memory task in a mouse model of a human risk allele of schizophrenia. During the task, mice first completed a sample phase, during which they were directed to one of the goal arms of a T-maze to receive a reward. After a delay of about 10 seconds, mice completed a choice phase (working memory-dependent), during which they had to choose the opposite goal arm in order to receive a reward. Researchers found that mice with the risk allele showed decreased phase locking of mPFC cells to hippocampal theta oscillations and lower hippocampal-prefrontal synchrony in the 4-6 Hz theta range compared to wild-type mice during choice phases of the task.

4.6 Conclusion, Future Directions, and Significance

Communication across the mPFC-RE-hippocampus network is important for spatial working memory and 3rd trimester AE is known to damage these structures. In addition to structural effects, our lab recently found that spatial working memory was impaired in adulthood in our 3rd trimester FASD rodent model. Here, we show that our rodent model of 3rd trimester AE also shows alterations in mPFC-hippocampus functional connectivity during decision making, as seen through a reduction in mPFC-hippocampus theta coherence at the choice point. Both structural damage and altered connectivity could explain impaired spatial working memory performance due to AE during the brain growth spurt. Findings of reduced mPFC-hippocampus

theta coherence during decision making in sessions performed by AE rats compared to SI rats expands upon previous behavioral and structural findings in our rodent model (Gursky et al., 2019, 2020, 2021; Kim et al., 2021; Smith et al., 2022).

We will continue collecting data to complete further analyses on the effects of developmental AE on mPFC-hippocampus functional connectivity, such as determining if there are effects related to delay length between trials and examining sex differences. By examining mPFC-hippocampus theta coherence at each delay length, we will determine if theta coherence is correlated to task performance in our AE and SI rats. Our DA task tests three different delay lengths within a session with varying working memory demand (10 seconds having the lowest and 60 seconds having the highest working memory demand). We expect that the need for mPFC-hippocampus interactions will change based on this demand. We predict that theta coherence and choice accuracy will not be correlated during 10 second delay trials in AE and SI rats, as both AE and SI rats improved across DA task sessions at this delay length during our previous behavioral experiment. It is possible that mPFC-hippocampus theta synchrony is not critical for correct task performance during this low spatial working memory demand condition, which could explain why the AE group did not show spatial working memory deficits during 10 second delay trials even though mPFC-hippocampus theta synchrony could have been reduced. It is also likely that theta coherence and choice accuracy during 60 second delay trials will not be correlated, as both the AE and SI groups performed poorly across sessions at this delay length during our behavioral experiment. In contrast, as the AE group, but not the SI group, previously showed impaired performance on 30 second delay trials across DA task sessions, we expect that mPFC-hippocampus theta synchrony is most important for successful task performance at this delay length. As a result, we predict that there will be a correlation between coherence and

choice accuracy during 30 second delay trials in AE and SI rats, with decreased coherence being correlated to poorer task performance in AE rats.

The current study also does not examine sex differences due to small sample size. As it has been shown that mPFC-originating axons in the RE were shorter in AE female rats (Smith et al., 2022), it is possible that there are also sex differences in mPFC-hippocampus synchrony between male and female rats. Finally, we will additionally explore therapeutic methods to reverse spatial working memory impairments in our rodent model of FASD.

The current findings lead to a better understanding of the effects of alcohol on mPFC-RE-hippocampus circuitry, which is necessary for spatial working memory and is damaged in a 3rd trimester FASD rodent model. This study additionally contributes to previous literature by exploring the effects of developmental AE on mPFC-hippocampus interactions, which could help explain cognitive deficits seen in adults with FASD.

REFERENCES

Ainge, J. A., van der Meer, M. A. A., Langston, R. F., & Wood, E. R. (2007). Exploring the role of context-dependent hippocampal activity in spatial alternation behavior. *Hippocampus*, *17*(10), 988–1002. https://doi.org/10.1002/hipo.20301

Bannerman, D. M., Grubb, M., Deacon, R. M. J., Yee, B. K., Feldon, J., & Rawlins, J. N. P. (2003). Ventral hippocampal lesions affect anxiety but not spatial learning. *Behavioural Brain Research*, *139*(1), 197–213. https://doi.org/10.1016/S0166-4328(02)00268-1

Bannerman, D. M., Rawlins, J. N. P., McHugh, S. B., Deacon, R. M. J., Yee, B. K., Bast, T., Zhang, W.-N., Pothuizen, H. H. J., & Feldon, J. (2004). Regional dissociations within the hippocampus—Memory and anxiety. *Neuroscience and Biobehavioral Reviews*, *28*(3), 273–283. https://doi.org/10.1016/j.neubiorev.2004.03.004

Bonthius, D. J., & West, J. R. (1991). Permanent neuronal deficits in rats exposed to alcohol during the brain growth spurt. *Teratology*, *44*(2), 147–163. https://doi.org/10.1002/tera.1420440203

Bragin, A., G Jando, Z Nadasdy, J Hetke, K Wise, & G Buzsaki. (1995). Gamma (40-100 Hz) oscillation in the hippocampus of the behaving rat. *The Journal of Neuroscience*, *15*(1), 47. https://doi.org/10.1523/JNEUROSCI.15-01-00047.1995

Buzsáki, G. (2002). Theta oscillations in the hippocampus. *Neuron*, *33*(3), 325–340. https://doi.org/10.1016/s0896-6273(02)00586-x

Buzsáki, G., Czopf, J., Kondákor, I., & Kellényi, L. (1986). Laminar distribution of hippocampal rhythmic slow activity (RSA) in the behaving rat: Current-source density analysis, effects of urethane and atropine. *Brain Research*, *365*(1), 125–137. https://doi.org/10.1016/0006-8993(86)90729-8

Buzsáki, G., Rappelsberger, P., & Kellényi, L. (1985). Depth profiles of hippocampal rhythmic slow activity ('theta rhythm') depend on behaviour. *Electroencephalography and Clinical Neurophysiology*, *61*(1), 77–88. https://doi.org/10.1016/0013-4694(85)91075-2

Candelaria-Cook, F. T., Schendel, M. E., Flynn, L., Hill, D. E., & Stephen, J. M. (2021). Altered Resting-State Neural Oscillations and Spectral Power in Children with Fetal Alcohol Spectrum Disorder. *Alcohol: Clinical and Experimental Research*, *45*(1), 117–130. https://doi.org/10.1111/acer.14502

Cassel, J.-C., Pereira de Vasconcelos, A., Loureiro, M., Cholvin, T., Dalrymple-Alford, J. C., & Vertes, R. P. (2013). The reuniens and rhomboid nuclei: Neuroanatomy, electrophysiological characteristics and behavioral implications. *Progress in Neurobiology*, *111*, 34–52. https://doi.org/10.1016/j.pneurobio.2013.08.006

Churchwell, J. C., & Kesner, R. P. (2011). Hippocampal-prefrontal dynamics in spatial working memory: Interactions and independent parallel processing. *Behavioural Brain Research*, *225*(2), 389–395. https://doi.org/10.1016/j.bbr.2011.07.045

Coles, C. (1994). Critical Periods for Prenatal Alcohol Exposure: Evidence From Animal and Human Studies. *Alcohol Health and Research World*, *18*(1), 22–29.

de Sanctis, L., Memo, L., Pichini, S., Tarani, L., & Vagnarelli, F. (2011). Fetal alcohol syndrome: New perspectives for an ancient and underestimated problem. *The Journal of Maternal-Fetal & Neonatal Medicine : The Official Journal of the European Association of Perinatal Medicine, the Federation of Asia and Oceania Perinatal Societies, the International Society of Perinatal Obstetricians*, *24 Suppl 1*, 34–37. https://doi.org/10.3109/14767058.2011.607576

Dobbing, J., & Sands, J. (1973). Quantitative growth and development of human brain. *Archives of Disease in Childhood*, *48*(10), 757–767. https://doi.org/10.1136/adc.48.10.757

Dobbing, J., & Sands, J. (1979). Comparative aspects of the brain growth spurt. *Early Human Development*, *3*(1), 79–83. https://doi.org/10.1016/0378-3782(79)90022-7

Fellows, B. J. (1967). Chance stimulus sequences for discrimination tasks. *Psychological Bulletin*, *67*(2), 87–92. https://doi.org/10.1037/h0024098

Girard, T. A., Xing, H.-C., Ward, G. R., & Wainwright, P. E. (2000). Early Postnatal Ethanol Exposure Has Long-Term Effects on the Performance of Male Rats in a Delayed Matching-to-Place Task in the Morris Water Maze. *Alcohol: Clinical and Experimental Research*, *24*(3), 300–306. https://doi.org/10.1111/j.1530-0277.2000.tb04611.x

Gordon, J. A. (2011). Oscillations and hippocampal–prefrontal synchrony. *Behavioural and Cognitive Neuroscience*, *21*(3), 486–491. https://doi.org/10.1016/j.conb.2011.02.012

Gursky, Z. H., Savage, L. M., & Klintsova, A. Y. (2019). Nucleus reuniens of the midline thalamus of a rat is specifically damaged after early postnatal alcohol exposure. *NeuroReport*, *30*(10). https://journals.lww.com/neuroreport/Fulltext/2019/07010/Nucleus_reuniens_of_the_midline_thalamus_of_a_rat.10.aspx

Gursky, Z. H., Savage, L. M., & Klintsova, A. Y. (2021). Executive functioning-specific behavioral impairments in a rat model of human third trimester binge drinking implicate prefrontal-thalamo-hippocampal circuitry in Fetal Alcohol Spectrum Disorders. *Behavioural Brain Research*, *405*, 113208. https://doi.org/10.1016/j.bbr.2021.113208

Gursky, Z. H., Spillman, E. C., & Klintsova, A. Y. (2020). Single-day Postnatal Alcohol Exposure Induces Apoptotic Cell Death and Causes long-term Neuron Loss in Rodent Thalamic Nucleus Reuniens. *Neuroscience*, *435*, 124–134. https://doi.org/10.1016/j.neuroscience.2020.03.046

Hallock, H. L., Arreola, A. C., Shaw, C. L., & Griffin, A. L. (2013). Dissociable roles of the dorsal striatum and dorsal hippocampus in conditional discrimination and spatial alternation T-maze tasks. *Neurobiology of Learning and Memory*, *100*, 108–116. https://doi.org/10.1016/j.nlm.2012.12.009

Hallock, H. L., Wang, A., & Griffin, A. L. (2016). Ventral Midline Thalamus Is Critical for Hippocampal–Prefrontal Synchrony and Spatial Working Memory. *The Journal of Neuroscience*, *36*(32), 8372. https://doi.org/10.1523/JNEUROSCI.0991-16.2016

Hamilton, G. F., Hernandez, I. J., Krebs, C. P., Bucko, P. J., & Rhodes, J. S. (2017). Neonatal alcohol exposure reduces number of parvalbumin-positive interneurons in the medial prefrontal cortex and impairs passive avoidance acquisition in mice deficits not rescued from exercise. *Neuroscience*, *352*, 52–63. https://doi.org/10.1016/j.neuroscience.2017.03.058

Hamilton, G. F., Whitcher, L. T., & Klintsova, A. Y. (2010). Postnatal binge-like alcohol exposure decreases dendritic complexity while increasing the density of mature spines in mPFC Layer II/III pyramidal neurons. *Synapse*, *64*(2), 127–135. https://doi.org/10.1002/syn.20711

Hinman, J. R., Penley, S. C., Long, L. L., Escabí, M. A., & Chrobak, J. J. (2011). Septotemporal variation in dynamics of theta: Speed and habituation. *Journal of Neurophysiology*, *105*(6), 2675–2686. https://doi.org/10.1152/jn.00837.2010

Hock, B. J., & Bunsey, M. D. (1998). Differential Effects of Dorsal and Ventral Hippocampal Lesions. *The Journal of Neuroscience*, *18*(17), 7027. https://doi.org/10.1523/JNEUROSCI.18-17-07027.1998

Hoover, W. B., & Vertes, R. P. (2007). Anatomical analysis of afferent projections to the medial prefrontal cortex in the rat. *Brain Structure and Function*, *212*(2), 149–179. https://doi.org/10.1007/s00429-007-0150-4

Hoyme, H. E., Kalberg, W. O., Elliott, A. J., Blankenship, J., Buckley, D., Marais, A.-S., Manning, M. A., Robinson, L. K., Adam, M. P., Abdul-Rahman, O., Jewett, T., Coles, C. D., Chambers, C., Jones, K. L., Adnams, C. M., Shah, P. E., Riley, E. P., Charness, M. E., Warren, K. R., & May, P. A. (2016). Updated Clinical Guidelines for Diagnosing Fetal Alcohol Spectrum Disorders. *Pediatrics*, *138*(2), e20154256. https://doi.org/10.1542/peds.2015-4256

Hyman, J. M., Zilli, E. A., Paley, A. M., & Hasselmo, M. E. (2010). Working Memory Performance Correlates with Prefrontal-Hippocampal Theta Interactions but not with Prefrontal Neuron Firing Rates. *Frontiers in Integrative Neuroscience*, *4*, 2. https://doi.org/10.3389/neuro.07.002.2010

Ikonomidou, C., Bittigau, P., Ishimaru, M. J., Wozniak, D. F., Koch, C., Genz, K., Price, M. T., Stefovska, V., Hörster, F., Tenkova, T., Dikranian, K., & Olney, J. W. (2000). Ethanol-Induced Apoptotic Neurodegeneration and Fetal Alcohol Syndrome. *Science*, *287*(5455), 1056–1060. https://doi.org/10.1126/science.287.5455.1056

Jay, T. M., & Witter, M. P. (1991). Distribution of hippocampal CA1 and subicular efferents in the prefrontal cortex of the rat studied by means of anterograde transport of Phaseolus vulgaris-leucoagglutinin. *Journal of Comparative Neurology*, *313*(4), 574–586. https://doi.org/10.1002/cne.903130404

Jayachandran, M., Tatiana D. Viena, Garcia, A., Vasallo Veliz, A., Leyva, S., Roldan, V., Vertes, R. P., & Allen, T. A. (2022). Reuniens transiently synchronizes memory networks at beta frequencies. BioRxiv, 2022.06.21.497087. https://doi.org/10.1101/2022.06.21.497087Jones, M. W., & Wilson, M. A. (2005). Theta Rhythms Coordinate Hippocampal–Prefrontal Interactions in a Spatial Memory Task. *PLOS Biology*, *3*(12), e402. https://doi.org/10.1371/journal.pbio.0030402

Kim, S., Klintsova, A. Y., & Griffin, A. L. (2021, November). *Spatial working memory is impaired in adult male and female rats after binge alcohol exposure in a third – trimester model of FASD* [Poster]. Society for Neuroscience, Virtual conference.

Krawczyk, M., Ramani, M., Dian, J., Florez, C. M., Mylvaganam, S., Brien, J., Reynolds, J., Kapur, B., Zoidl, G., Poulter, M. O., & Carlen, P. L. (2016). Hippocampal hyperexcitability in fetal alcohol spectrum disorder: Pathological sharp waves and excitatory/inhibitory synaptic imbalance. Experimental Neurology, 280, 70–79. https://doi.org/10.1016/j.expneurol.2016.03.013

Lawrence, R. C., Otero, N. K. H., & Kelly, S. J. (2012). Selective effects of perinatal ethanol exposure in medial prefrontal cortex and nucleus accumbens. *Neurotoxicology and Teratology*, *34*(1), 128–135. https://doi.org/10.1016/j.ntt.2011.08.002

Layfield, D. M., Patel, M., Hallock, H., & Griffin, A. L. (2015). Inactivation of the nucleus reuniens/rhomboid causes a delay-dependent impairment of spatial working memory. *Neurobiology of Learning and Memory*, *125*, 163–167. https://doi.org/10.1016/j.nlm.2015.09.007

Lee, I., & Kesner, R. P. (2003). Time-Dependent Relationship between the Dorsal Hippocampus and the Prefrontal Cortex in Spatial Memory. *The Journal of Neuroscience*, *23*(4), 1517. https://doi.org/10.1523/JNEUROSCI.23-04-01517.2003

Little, G., Reynolds, J., & Beaulieu, C. (2018). Altered Functional Connectivity Observed at Rest in Children and Adolescents Prenatally Exposed to Alcohol. *Brain Connectivity*, *8*(8), 503–515. https://doi.org/10.1089/brain.2017.0572

Livy, D. J., Miller, E. K., Maier, S. E., & West, J. R. (2003). Fetal alcohol exposure and temporal vulnerability: Effects of binge-like alcohol exposure on the developing rat hippocampus. *Neurotoxicology and Teratology*, *25*(4), 447–458. https://doi.org/10.1016/s0892-0362(03)00030-8

Long, L., Hinman, J., Chen, C.-M., Escabí, M., & Chrobak, J. (2014). Theta Dynamics in Rat: Speed and Acceleration across the Septotemporal Axis. *PloS One*, *9*, e97987. https://doi.org/10.1371/journal.pone.0097987

Maharjan, D. M., Dai, Y. Y., Glantz, E. H., & Jadhav, S. P. (2018). Disruption of dorsal hippocampal – prefrontal interactions using chemogenetic inactivation impairs spatial learning. *Neurobiology of Learning and Memory*, *155*, 351–360. https://doi.org/10.1016/j.nlm.2018.08.023

May, P. A., Chambers, C. D., Kalberg, W. O., Zellner, J., Feldman, H., Buckley, D., Kopald, D., Hasken, J. M., Xu, R., Honerkamp-Smith, G., Taras, H., Manning, M. A., Robinson, L. K., Adam, M. P., Abdul-Rahman, O., Vaux, K., Jewett, T., Elliott, A. J., Kable, J. A., … Hoyme, H. E. (2018). Prevalence of Fetal Alcohol Spectrum Disorders in 4 US Communities. *JAMA*, *319*(5), 474–482. https://doi.org/10.1001/jama.2017.21896

McFarland, W. L., Teitelbaum, H., & Hedges, E. K. (1975). Relationship between hippocampal theta activity and running speed in the rat. *Journal of Comparative and Physiological Psychology*, *88*(1), 324–328. https://doi.org/10.1037/h0076177

Milbocker, K. A., Campbell, T. S., Collins, N., Kim, S., Smith, I. F., Roth, T. L., & Klintsova, A. Y. (2021). Glia-Driven Brain Circuit Refinement Is Altered by Early-Life Adversity: Behavioral Outcomes. Frontiers in Behavioral Neuroscience, 15. https://www.frontiersin.org/articles/10.3389/fnbeh.2021.786234Mitra, P. (2007). *Observed brain dynamics*. Oxford University Press.

Moser, E., Moser, M.-B., & Andersen, P. (1993). Spatial learning impairment parallels the magnitude of dorsal hippocampal lesions, but is hardly present following ventral lesions. *The Journal of Neuroscience*, *13*(9), 3916. https://doi.org/10.1523/JNEUROSCI.13-09-03916.1993

Moser, M.-B., & Moser, E. I. (1998). Functional differentiation in the hippocampus. *Hippocampus*, *8*(6), 608–619. https://doi.org/10.1002/(SICI)1098-1063(1998)8:6<608::AID-HIPO3>3.0.CO;2-7

Murawski, N. J., Klintsova, A. Y., & Stanton, M. E. (2012). Neonatal alcohol exposure and the hippocampus in developing male rats: Effects on behaviorally induced CA1 c-Fos expression, CA1 pyramidal cell number, and contextual fear conditioning. *Neuroscience*, *206*, 89–99. https://doi.org/10.1016/j.neuroscience.2012.01.006

O'Neill, P.-K., Gordon, J. A., & Sigurdsson, T. (2013). Theta oscillations in the medial prefrontal cortex are modulated by spatial working memory and synchronize with the hippocampus through its ventral subregion. *The Journal of Neuroscience : The Official Journal of the Society for Neuroscience*, *33*(35), 14211–14224. https://doi.org/10.1523/JNEUROSCI.2378-13.2013

Otero, N. K. H., Thomas, J. D., Saski, C. A., Xia, X., & Kelly, S. J. (2012). Choline Supplementation and DNA Methylation in the Hippocampus and Prefrontal Cortex of Rats Exposed to Alcohol During Development. *Alcohol: Clinical and Experimental Research*, *36*(10), 1701–1709. https://doi.org/10.1111/j.1530-0277.2012.01784.x

Rabinovici, G. D., Stephens, M. L., & Possin, K. L. (2015). Executive dysfunction. *Continuum (Minneapolis, Minn.)*, *21*(3 Behavioral Neurology and Neuropsychiatry), 646–659. https://doi.org/10.1212/01.CON.0000466658.05156.54

Roebuck, T. M., Mattson, S. N., & Riley, E. P. (1998). A review of the neuroanatomical findings in children with fetal alcohol syndrome or prenatal exposure to alcohol. *Alcoholism,*

Clinical and Experimental Research, *22*(2), 339–344. https://doi.org/10.1111/j.1530-0277.1998.tb03658.x

Rosene, D. L., Roy, N. J., & Davis, B. J. (1986). A cryoprotection method that facilitates cutting frozen sections of whole monkey brains for histological and histochemical processing without freezing artifact. *The Journal of Histochemistry and Cytochemistry : Official Journal of the Histochemistry Society*, *34*(10), 1301–1315. https://doi.org/10.1177/34.10.3745909

Semple, B. D., Blomgren, K., Gimlin, K., Ferriero, D. M., & Noble-Haeusslein, L. J. (2013). Brain development in rodents and humans: Identifying benchmarks of maturation and vulnerability to injury across species. Progress in Neurobiology, 106–107, 1–16. https://doi.org/10.1016/j.pneurobio.2013.04.001

Sharott, A. (2014). Local Field Potential, Methods of Recording. In D. Jaeger & R. Jung (Eds.), *Encyclopedia of Computational Neuroscience* (pp. 1–3). Springer New York. https://doi.org/10.1007/978-1-4614-7320-6_723-1

Shaw, C. L., Watson, G. D. R., Hallock, H. L., Cline, K. M., & Griffin, A. L. (2013). The role of the medial prefrontal cortex in the acquisition, retention, and reversal of a tactile visuospatial conditional discrimination task. *Behavioural Brain Research*, *236*, 94–101. https://doi.org/10.1016/j.bbr.2012.08.024

Sheremet, A., Burke, S. N., & Maurer, A. P. (2016). Movement Enhances the Nonlinearity of Hippocampal Theta. The Journal of Neuroscience, 36(15), 4218. https://doi.org/10.1523/JNEUROSCI.3564-15.2016

Sigurdsson, T., Stark, K. L., Karayiorgou, M., Gogos, J. A., & Gordon, J. A. (2010). Impaired hippocampal–prefrontal synchrony in a genetic mouse model of schizophrenia. *Nature*, *464*(7289), 763–767. https://doi.org/10.1038/nature08855

Smith, I. F., Gursky, Z. H., & Klintsova, A. Y. (2022). Representation of prefrontal axonal efferents in the thalamic nucleus reuniens in a rodent model of fetal alcohol exposure during third trimester. *Frontiers in Behavioral Neuroscience*. Natural Science Collection; Publicly Available Content Database. https://doi.org/10.3389/fnbeh.2022.993601

Spellman, T., Rigotti, M., Ahmari, S. E., Fusi, S., Gogos, J. A., & Gordon, J. A. (2015). Hippocampal–prefrontal input supports spatial encoding in working memory. *Nature*, *522*(7556), 309–314. https://doi.org/10.1038/nature14445

Su, H.-S., & Bentivoglio, M. (1990). Thalamic midline cell populations projecting to the nucleus accumbens, amygdala, and hippocampus in the rat. *Journal of Comparative Neurology*, *297*(4), 582–593. https://doi.org/10.1002/cne.902970410

Tang, S., Xu, S., Gullapalli, R. P., & Medina, A. E. (2018). Effects of Early Alcohol Exposure on Functional Organization and Microstructure of a Visual-Tactile Integrative Circuit. *Alcoholism, Clinical and Experimental Research*, *42*(4), 727–734. https://doi.org/10.1111/acer.13611

Thomas, J. D., Wasserman, E. A., West, J. R., & Goodlett, C. R. (1996). Behavioral deficits induced by bingelike exposure to alcohol in neonatal rats: Importance of developmental timing and number of episodes. *Developmental Psychobiology*, *29*(5), 433–452. https://doi.org/10.1002/(SICI)1098-2302(199607)29:5<433::AID-DEV3>3.0.CO;2-P

Tran, T. D., & Kelly, S. J. (2003). Critical periods for ethanol-induced cell loss in the hippocampal formation. *Neurotoxicology and Teratology*, *25*(5), 519–528. https://doi.org/10.1016/S0892-0362(03)00074-6

Varela, C., Kumar, S., Yang, J. Y., & Wilson, M. A. (2014). Anatomical substrates for direct interactions between hippocampus, medial prefrontal cortex, and the thalamic nucleus reuniens. *Brain Structure & Function*, *219*(3), 911–929. https://doi.org/10.1007/s00429-013-0543-5

Vertes, R. P. (2002). Analysis of projections from the medial prefrontal cortex to the thalamus in the rat, with emphasis on nucleus reuniens. *Journal of Comparative Neurology*, *442*(2), 163–187. https://doi.org/10.1002/cne.10083

Vertes, R. P., Hoover, W. B., Do Valle, A. C., Sherman, A., & Rodriguez, J. J. (2006). Efferent projections of reuniens and rhomboid nuclei of the thalamus in the rat. *Journal of Comparative Neurology*, *499*(5), 768–796. https://doi.org/10.1002/cne.21135

Vertes, R. P., Hoover, W. B., Szigeti-Buck, K., & Leranth, C. (2007). Nucleus reuniens of the midline thalamus: Link between the medial prefrontal cortex and the hippocampus. *Brain Research Bulletin*, *71*(6), 601–609. https://doi.org/10.1016/j.brainresbull.2006.12.002

Wang, G.-W., & Cai, J.-X. (2006). Disconnection of the hippocampal–prefrontal cortical circuits impairs spatial working memory performance in rats. *Behavioural Brain Research*, *175*(2), 329–336. https://doi.org/10.1016/j.bbr.2006.09.002

Whishaw, I. Q., & Vanderwolf, C. H. (1973). Hippocampal EEG and behavior: Change in amplitude and frequency of RSA (Theta rhythm) associated with spontaneous and learned movement patterns in rats and cats. *Behavioral Biology*, *8*(4), 461–484. https://doi.org/10.1016/S0091-6773(73)80041-0

Whitcher, L. T., & Klintsova, A. Y. (2008). Postnatal binge-like alcohol exposure reduces spine density without affecting dendritic morphology in rat mPFC. *Synapse*, *62*(8), 566–573. https://doi.org/10.1002/syn.20532

Williams, J. F., Smith, V. C., & COMMITTEE ON SUBSTANCE ABUSE. (2015). Fetal Alcohol Spectrum Disorders. *Pediatrics*, *136*(5), e1395-1406. https://doi.org/10.1542/peds.2015-3113

Wilson, D. A., Peterson, J., Basavaraj, B. S., & Saito, M. (2011). Local and Regional Network Function in Behaviorally Relevant Cortical Circuits of Adult Mice Following Postnatal Alcohol Exposure. *Alcohol: Clinical and Experimental Research*, *35*(11), 1974–1984. https://doi.org/10.1111/j.1530-0277.2011.01549.x

Wozniak, D. F., Hartman, R. E., Boyle, M. P., Vogt, S. K., Brooks, A. R., Tenkova, T., Young, C., Olney, J. W., & Muglia, L. J. (2004). Apoptotic neurodegeneration induced by ethanol in neonatal mice is associated with profound learning/memory deficits in juveniles followed by progressive functional recovery in adults. *Neurobiology of Disease*, *17*(3), 403–414. https://doi.org/10.1016/j.nbd.2004.08.006

Wozniak, J. R., Mueller, B. A., Mattson, S. N., Coles, C. D., Kable, J. A., Jones, K. L., Boys, C. J., Lim, K. O., Riley, E. P., Sowell, E. R., & the CIFASD. (2017). Functional connectivity abnormalities and associated cognitive deficits in fetal alcohol Spectrum disorders (FASD). *Brain Imaging and Behavior*, *11*(5), 1432–1445. https://doi.org/10.1007/s11682-016-9624-4